

# UC Irvine

## UC Irvine Previously Published Works

### Title

Tissue hemoglobin monitoring of progressive central hypovolemia in humans using broadband diffuse optical spectroscopy

### Permalink

<https://escholarship.org/uc/item/69z0666g>

### Journal

Journal of Biomedical Optics, 13(6)

### ISSN

1083-3668

### Authors

Lee, Jangwoen  
Kim, Jae G  
Mahon, Sari  
[et al.](#)

### Publication Date

2008

### DOI

10.1117/1.3041712

### Copyright Information

This work is made available under the terms of a Creative Commons Attribution License, available at <https://creativecommons.org/licenses/by/4.0/>

Peer reviewed



Published in final edited form as:

*J Biomed Opt.* 2008 ; 13(6): 064027. doi:10.1117/1.3041712.

## Tissue hemoglobin monitoring of progressive central hypovolemia in humans using broadband diffuse optical spectroscopy

**Jangwoen Lee,**

University of California, Irvine, Beckman Laser Institute and Medical Clinic, 1002 Health Sciences Road East, Irvine, California 92612

**Jae G. Kim,**

University of California, Irvine, Beckman Laser Institute and Medical Clinic, 1002 Health Sciences Road East, Irvine, California 92612

**Sari Mahon,**

University of California, Irvine, Beckman Laser Institute and Medical Clinic, 1002 Health Sciences Road East, Irvine, California 92612

**Bruce J. Tromberg,**

University of California, Irvine, Beckman Laser Institute and Medical Clinic, 1002 Health Sciences Road East, Irvine, California 92612

**Kathy L. Ryan,**

U.S. Army Institute of Surgical Research, Fort Sam Houston, Texas 78234

**Victor A. Convertino,**

U.S. Army Institute of Surgical Research, Fort Sam Houston, Texas 78234

**Caroline A. Rickards,**

U.S. Army Institute of Surgical Research, Fort Sam Houston, Texas 78234

**Kathryn Osann, and**

University of California, Irvine, Department of Medicine, 1002 Health Sciences Road East, Irvine, California 92612

**Matthew Brenner**

University of California, Irvine, Beckman Laser Institute and Medical Clinic, 1002 Health Sciences Road East, Irvine California 92612

University of California, Irvine Medical Center, Pulmonary and Critical Care Division, Building 53, Room 119, 101 City Drive South, Orange, California 92868

### Abstract

---

© 2008 Society of Photo-Optical Instrumentation Engineers.

Address all correspondence to: Jangwoen Lee, Ph.D., Beckman Laser Institute and Medical Clinic, University of California, Irvine, 1002 Health Sciences Road East, Irvine, CA 92612; Tel: 949-824-0524 Fax: 949-824-6969; jangwl@uci.edu; or Matt Brenner, M.D., Professor of Medicine, Pulmonary and Critical Care Division, UC Irvine Medical Center, Bldg. 53, Rm. 119, 101 City Drive South, Orange, CA 92868; Tel: 714 456-5150; Fax: 714 456-8349; mbrenner@uci.edu.

We demonstrate noninvasive near-infrared diffuse optical spectroscopy (DOS) measurements of tissue hemoglobin contents that can track progressive reductions in central blood volume in human volunteers. Measurements of mean arterial blood pressure (MAP), heart rate (HR), stroke volume (SV), and cardiac output (Q) are obtained in ten healthy human subjects during baseline supine rest and exposure to progressive reductions of central blood volume produced by application of lower body negative pressure (LBNP). Simultaneous quantitative noninvasive measurements of tissue oxyhemoglobin (OHb), deoxyhemoglobin (RHb), total hemoglobin concentration (THb), and tissue hemoglobin oxygen saturation ( $S_tO_2$ ) are performed throughout LBNP application using broadband DOS. As progressively increasing amounts of LBNP are applied, HR increases, and MAP, SV, and Q decrease ( $p < 0.001$ ). OHb,  $S_tO_2$ , and THb decrease ( $p < 0.001$ ) in correlation with progressive increases in LBNP, while tissue RHb remained relatively constant ( $p = 0.378$ ). The average fractional changes from baseline values in DOS OHb (fOHb) correlate closely with independently measured changes in SV ( $r^2 = 0.95$ ) and Q ( $r^2 = 0.98$ ) during LBNP. Quantitative noninvasive broadband DOS measurements of tissue hemoglobin parameters of peripheral perfusion are capable of detecting progressive reductions in central blood volume, and appear to be sensitive markers of early hypoperfusion associated with hemorrhage as simulated by LBNP.

## Keywords

hemorrhagic shock; lower body negative pressure; hemodynamic decompensation

---

## 1 Introduction

Hemorrhage resulting from injuries is the leading cause of preventable mortality in both civilian and military trauma settings, and has been reported to be responsible for up to 80% of civilian trauma deaths and 50% of combat-related deaths.<sup>1,2</sup> Outcomes might be improved if the severity of blood loss is recognized early in the prehospital setting.<sup>3,4</sup> Thus, new approaches for early detection of blood loss in prehospital and combat environments, as well as in hospitalized patients, are essential in civilian and military medicine.<sup>5</sup>

Several criteria have been developed in an attempt to help determine injury severity, mode of transport, and treatment prioritization of trauma patients.<sup>6-13</sup> However, most of these existing assessment tools currently rely on standard vital signs data (e.g., blood pressure and heart rate) because of the ready availability of these parameters on site. The sensitivity and specificity of such assessment tools in detecting early hemorrhage is limited by the complex, dynamic physiology and compensatory reflex responses of the hemorrhaging patient, particularly in the trauma setting.<sup>14-17</sup> During early volume loss, reflex cardiovascular and neurohormonal mechanisms act to maintain normal arterial pressures, with only mild tachycardia being apparent. Specifically, autonomically mediated reflexes initiate strong sympathetic responses that result in intense vasoconstriction and help defend against severe hypotension.<sup>15,16</sup> Thus, the degree of blood volume loss can be masked, particularly in the critical early stages following injury, and subsequently may not provide important information needed for decision support in recognition of the severity of injury.

A number of other methods for assessment of the degree of hemorrhage have also been proposed, including pulse pressure monitoring, end tidal carbon dioxide partial pressure monitoring, and assessment of heart rate variability.<sup>12,18–25</sup> The role of each of these variables alone and in combination continues to be investigated.

Thus, at this time, the process and complex practice of prehospital trauma care, field triage, and in-hospital recognition of early hemorrhage may be significantly advanced by developing novel noninvasive, physiologic measurement capabilities that could provide more accurate indicators of early blood volume loss and impending circulatory collapse.<sup>5</sup>

A recently developed technology, broadband diffuse optical spectroscopy (DOS), has the potential to noninvasively assess the physiologic changes associated with early hemorrhage-induced reductions in tissue perfusion.<sup>26–33</sup> Broadband DOS is a near-infrared (NIR) optical spectroscopic approach that can measure complex tissue scattering induced light signal attenuation, and use this information in the determination of broadband NIR absorption spectra in tissues. This information can then be translated into quantitative measurements of the NIR absorbing constituents of the tissue, including oxyhemoglobin (OHb), deoxyhemoglobin (RHb), total hemoglobin concentration (THb), and tissue hemoglobin oxygen saturation ( $S_tO_2$ ), as well as tissue water and lipid concentrations.

In this study, we investigated the ability of broadband DOS to quantitatively detect changes in peripheral perfusion occurring in early central blood volume reduction induced by lower body negative pressure (LBNP) in healthy human volunteers. In the event of hemorrhagic hypovolemia, most blood volume loss comes from constriction of the arterials and primarily veins. In addition, there is reduction in intravascular hematocrit over time with hypovolemic hemorrhage. A decrease in venous volume leads to a decrease in venous return and preload resulting in a decrease in cardiac output. LBNP has been shown to mimic the acute hemodynamic and autonomic responses associated with actual hemorrhage.<sup>15,25,34–37</sup> In the present investigation, we compared noninvasive broadband DOS measures of OHb, RHb, THb, and  $S_tO_2$  to standard measures of heart rate, mean arterial pressure, stroke volume, and cardiac output, at rest and during graded exposure to LBNP, to test the hypothesis that broadband DOS measured changes directly correlate with reductions in central blood volume in humans exposed to a noninvasive model of progressive central hypovolemia.

## 2 Materials and Methods

### 2.1 Human Subject Approval and Consent

This protocol was approved by the Institutional Review Boards at the Institute of Surgical Research, Fort Sam Houston, San Antonio, Texas, the U.S. Department of Defense, and at University of California, Irvine. Written informed consent was obtained from all participants in accordance with Federal, Department of Defense, and State Regulations. The LBNP protocol used has been previously described.<sup>15,25,34–37</sup>

### 2.2 Subjects

13 healthy nonsmoking subjects were recruited to participate and ten subjects completed the procedures (6 males, 4 females) with mean $\pm$ SEM age of 23 $\pm$ 1 yr, body weight of 77.3 $\pm$ 4.3

kg, and height of  $178\pm 4$  cm. Data from three additional subjects were excluded due to equipment malfunctions (2 male subjects) and a female subject terminated the procedure before reaching a true presyncopal stage. A complete medical history and physical examination were obtained for each of the potential subjects. In addition, female subjects underwent an initial urine test prior to experimentation to ensure that they were not pregnant. Subjects maintained their normal sleep pattern, refrained from exercise, and abstained from caffeine and other autonomic stimulants such as prescription or nonprescription drugs for at least 24 h prior to each experimental protocol unless cleared by the physician medical screener to continue taking the medications.

During an orientation session that preceded each experiment, all subjects received a verbal briefing and a written description of all procedures and risks associated with the experiments, and were made familiar with the laboratory, the protocol, and procedures.

### 2.3 Lower Body Negative Pressure Model of Central Hypovolemia

LBNP was used in the present investigation as an experimental tool to simulate loss of central blood volume in humans during hemorrhage.<sup>34,36</sup> With the use of a neoprene skirt designed to form an airtight seal between the subject and the chamber, the application of negative pressure to the lower body (below the iliac crest) with the subject in a supine position results in a redistribution of blood away from the upper body (head and heart) to the lower extremities and abdomen [Fig. 1(a)]. Thus, this model provides a unique method of investigating conditions of controlled, progressive, experimentally induced hypovolemic hypotension. Absolute equivalence between the magnitude of negative pressure applied and the magnitude of actual blood loss cannot be determined at this time, but review of both human and animal data reveal ranges of effective blood loss (or fluid displacement) caused by LBNP.<sup>34</sup> Figure 1(b) illustrates the standard LBNP protocol.

### 2.4 Experimental Protocol

All subjects were instrumented with an infrared finger photoplethysmograph (Finometer® Blood Pressure Monitor, TNO-TPD Biomedical Instrumentation, Amsterdam, The Netherlands) and an electrocardiogram to record beat-by-beat arterial pressures and heart rate (HR). The Finometer® blood pressure cuff was placed on the middle finger of the left hand, which in turn was placed at heart level. Very accurate measurements compared to directly measured intra-arterial pressures during various physiological maneuvers have been demonstrated with this device.<sup>38-40</sup> Mean arterial pressure (MAP) was calculated by dividing the sum of systolic blood pressure (SBP) and twice diastolic blood pressure (DBP) by three. Stroke volume (SV) was measured noninvasively with the previously described thoracic impedance measurement method.<sup>41</sup> Thoracic electrical bioimpedance was measured with an HIC-2000 Bio-Electric Impedance Cardiograph (Bio-Impedance Technology, Chapel Hill, North Carolina). The thoracic electrical bioimpedance technique is based on the resistance changes in the thorax to a low-intensity (4 mA), high-frequency (70 kHz) alternating current applied to the thorax by two surface electrodes placed at the root of the neck and two surface electrodes placed at the xiphoid process at the midaxillary line. Ventricular SV was determined with the partly empirical formula:  $SV$  (in ml) =  $\rho \times (L/Z_0)^2 \times LVET \times (dZ/dt)$ , where  $\rho$  (in ohm/cm) is the blood resistivity, a constant of 135

ohms/cm *in vivo*;  $L$  (in cm) is the mean distance between the inner band electrodes (front and back);  $Z_0$  (in ohms) is the average thoracic background impedance; LVET (in seconds) is the left ventricular ejection time; and  $(dZ/dt)$  is the maximum height of the  $dZ/dt$  peak measured from the zero line.<sup>42</sup> Correlation coefficients of 0.70 to 0.93 have been reported in SV measurements simultaneously made with thoracic electrical bioimpedance and thermodilution techniques.<sup>41</sup> Cardiac output (Q) was calculated as SV multiplied by HR.

Each subject underwent exposure to the LBNP protocol designed to test their tolerance to experimentally induced hypotensive hypovolemia. The LBNP protocol consisted of a 5-min rest period (0 mmHg) followed by 5 min of chamber decompression to -15, -30, -45, and -60 mmHg, and additional increments of -10 mmHg every 5 min until the onset of hemodynamic decompensation or the completion of 5 min at -100 mmHg [Fig. 1(b)]. Hemodynamic decompensation was defined by a precipitous fall in SBP greater than 15 mmHg, coincident with the onset of presyncopal symptoms such as gray-out (loss of vision), sweating, nausea, or dizziness.

## 2.5 Broadband Diffuse Optical Spectroscopy

Diffuse optical spectroscopy instrumentation, specifications, and application have been previously described as well.<sup>26-31,43-45</sup> A prototype multiwavelength, frequency domain instrument (FDPM) we designed and constructed in our laboratory was combined with a steady-state NIR spectrometer to create the DOS device for the noninvasive *in-vivo* assessment of changing tissue hemoglobin contents.<sup>46,47</sup> The broadband DOS system we designed employs six laser diodes (661, 681, 783, 805, and 823, 850 nm) and a fiber-coupled avalanche photo diode (APD) detector (Hamamatsu high-speed APD module C5658, Bridgewater, New Jersey). The APD detects the intensity-modulated diffuse reflectance signal at modulation frequencies between 50 to 300 MHz after propagating through the tissue. The absorption and reduced scattering coefficients are measured directly at each of the six laser diode wavelengths using the frequency-dependent phase and amplitude data.<sup>46-48</sup> The reduced scattering coefficient is calculated as a function of wavelength throughout the NIR by fitting a power law to these six reduced scattering coefficients.<sup>49-51</sup> The steady-state acquisition is a broadband reflectance measurement from 650 to 1000 nm that follows the FD measurements using a tungsten-halogen light source (Ocean Optics HL-2000, Dunedin, Florida) and a spectrometer (BWTEK BTC611E, Newark, Delaware). The broadband DOS probe houses a fiber-coupled APD detector with a rectangular contact surface ( $9.14 \pm 5.33$  cm). The broadband DOS probe was placed on the right bicep securely and mechanically throughout the experiment. The bicep muscle was chosen for the measurement site mainly because of easy accessibility and the availability of large muscle volume. The source/detector separation of FD and steady-state fiber optic probes was set at 25 mm at default, but it was adjusted up to 35 mm according to detection signals on an individual basis. The intensity of the steady-state (SS) reflectance measurements are calibrated to the FD values of absorption and scattering to establish the *absolute* reflectance intensity. Finally, the tissue concentrations of OHb, RHb, lipid, and water are calculated by a linear least-squares fit of the wavelength-dependent extinction coefficient spectra of each chromophore. We used OHb and RHb absorption spectra reported by Zijlstra, Buursma, and Assendelft<sup>52</sup> for the subsequent fitting and analysis. We

used the square bracket (i.e., [OHb], [RHb], and [THb]) to represent the tissue concentrations of chromophores.

## 2.6 Statistical Analysis

Subjects reached hemodynamic decompensation (i.e., maximal LBNP tolerance) at different absolute LBNP levels based on their individual physiological responses. Because cardiovascular decompensation occurs at different LBNP levels for individual subjects,<sup>53</sup> we routinely standardize the analysis by normalizing each individual's data to equal fractions between 0% LBNP tolerance (baseline) and 100% LBNP tolerance (the level at which the LBNP protocol was terminated as a result of impending hemodynamic decompensation).<sup>15,18,35,37</sup> This approach considers the data from all subjects relative to their maximum capacity to tolerate central hypovolemia.

Cardiovascular variables were averaged over the last 3 min of each LBNP level. One-way (LBNP level) randomized block (subjects) analysis of variance for repeated measures was used for comparison of outcome variables. When statistical differences were found, Bonferroni-corrected comparisons with baseline measurements were performed to determine the first level of LBNP that could be distinguished statistically from baseline. Similar analyses were carried out with DOS variables. All data are presented as mean  $\pm$  standard error (SE), and exact p values are presented for all comparisons. A difference  $p < 0.05$  was considered significant.

## 3 Results

The mean values at baseline and 100% LBNP tolerance for all variables are displayed in Table 1. Absolute values of cardiovascular variables (MAP, HR, SV, and Q) are listed as well as both absolute values (RHb, OHb, THb), and fractional changes from respective baseline values (fRHb, fOHb, and fTHb, respectively) are calculated as shown:

$$fVar = \frac{([C]_{LBNP}^{var} - [C]_{base}^{var})}{[C]_{base}^{var}} \times 100(\%),$$

where  $[C]_{LBNP}^{var}$  and  $[C]_{base}^{var}$  are concentrations of variable at a specific LBNP% and baseline (0% LBNP), respectively. The lipid fraction is the lipid mass density ( $\text{g mL}^{-1}$ ) in tissue relative to a lipid mass density of  $0.9 \text{ g mL}^{-1}$ , and the water fraction is the water concentration in tissue relative to the concentration of pure water (55.6 M). Among outcome variables, HR, MAP, SV, Q,  $S_tO_2$ ,  $S_tO_2$ , fOHb, and fTHb exhibited statistically significant alterations between baseline and presyncope (100% LBNP tolerance) in terms of population mean.

Figure 2 shows HR, SV, MAP, and Q during LBNP. Repeated measures analysis of variance (ANOVA) showed that the effect of progressive LBNP is significant for HR, MAP, SV, and Q within subjects ( $p < 0.001$ ). When compared with baseline values, SV showed the earliest changes ( $p = 0.032$  at 40% maximal LBNP), while MAP did not decline significantly until 100% LBNP ( $p = 0.012$ ).

Figure 3 graphically shows absolute values of [RHb], [OHb], [THb], and  $S_tO_2$  during LBNP applications. [OHb],  $S_tO_2$ , and [THb] decreased with progressive increases in LBNP ( $p < 0.001$ ), while tissue [RHb] remained relatively constant ( $p = 0.378$ ).

Large variations in baseline and subsequent absolute tissue hemoglobin concentrations among subjects at different LBNP levels are expected, since interrogating tissue volumes are inherently different from subject to subject. For instance, lipid and water fraction measured by broadband DOS ranged from 24 to 71% and 24 to 72%, respectively. These variations in part explain the wide range of (THb) from 35 to 114  $\mu\text{M}$  at the baseline. However, variability in baseline broadband DOS variables can be accounted for by normalizing to fractional changes relative to baseline values. Figure 4 graphically depicts fractional changes in [RHb], [OHb], [THb], from baseline concentrations and the changes in  $S_tO_2$  from baseline values. fOHb decreased significantly at 20% LBNP ( $p = 0.004$ ), and fTHb and  $S_tO_2$  at 60% LBNP ( $p = 0.008$ ). fRHb did not change significantly from the baseline value. The ranges of changes in fOHb and fTHb were far greater than that of  $S_tO_2$  ( $-24.7$  and  $-21.6\%$  versus  $-3.7\%$  at 100% LBNP, respectively).

To identify DOS variables that correlate with cardiovascular variables, simple Pearson correlation coefficients ( $r^2$ ) were calculated among variables shown in Figs. 2–4. The results are listed in Table 2. MAP and HR correlated poorly with all DOS variables, while RHb and fRHb correlated poorly with cardiovascular variables. On the other hand, [OHb], [THb], fOHb, fTHb,  $S_tO_2$ , and  $S_tO_2$  showed good correlations with SV and Q ( $r^2 > 0.88$ ).

Figure 5(a) illustrates typical time course plots of DOS fOHb, MAP, and SV from a single subject (male, 24 yr, 191 cm, 73 kg). MAP and SV data points were extracted from the continual Finometer measurement and compared with DOS fOHb measurement time points for the comparison. Figure 5(b) shows close correlations between fOHb and SV (left y axis) and Q (right y axis) from all ten subjects.

## 4 Discussion

Advances in methods for early detection of reduced central blood volume resulting from hemorrhage are essential for improvement in civilian and military trauma and critical care. Early changes that have been shown to occur with reduction in central blood volume include reduction in cardiac output and decreased delivery of oxygen in the blood to peripheral tissues.<sup>16,17,34,54</sup> In this study, we were able to demonstrate the ability of noninvasive broadband DOS to detect early changes in central blood volume induced by progressive LBNP. The changes detected correlated closely with independently measured stroke volume changes and with the degree of applied LBNP. The ability of broadband DOS to determine the extent of scattering-induced light attenuation provides the distinct advantage over existing technologies of quantitatively and continually measuring [THb], [OHb], [RHb], as well as  $S_tO_2$ .

During blood loss events in actual hemorrhage, [THb] measured by broadband DOS using the animal model decreases due to a combination of vasoconstriction and decreased intravascular hematocrit (i.e., intravascular hemoglobin).<sup>31,33</sup> While with LBNP-induced



decreases in central volume, it is the vasoconstriction component of decreased tissue hemoglobin that can be detected, since intravascular hematocrit does not change significantly. In addition, during hemorrhage, the tissue [OHb] decreases due to vasoconstriction, decreased intravascular hematocrit, and increased conversion of OHb to RHb by the underperfused tissues. Because DOS measures the average concentration over the region of interrogation, the components in the arterioles, capillaries, and venules are included in the measurement. Contributions from the reduction in intravascular volume from vasoconstriction and the increased conversion of OHb to RHb are detected.<sup>31</sup>

From our previous study, in contrast to [THb] and [OHb], [RHb] levels did not change significantly during progressive reductions in central blood volume, because the decreased deoxyhemoglobin resulting from vasoconstriction (and decreased hematocrit in the case of hemorrhage) is offset by increased deoxyhemoglobin due to increased conversion from oxyhemoglobin to deoxyhemoglobin at the tissue level.<sup>31</sup>

Thus, despite some obvious differences between trauma-induced hemorrhage and progressive LBNP, the overall pattern of tissue perfusion effects are similar, and the important early changes in tissue level perfusion effects are shown to be readily detectable by broadband DOS.

A number of other NIR spectroscopic approaches have been developed and tested in hemorrhage and central hypovolemic models. Recently, average tissue hemoglobin oxygen saturation from a commercial continuous-wave NIRS device (Hutchinson Technologies) was compared with a prototype sensor that determines muscle tissue hemoglobin oxygen saturation and muscle oxygen partial pressure determination using the same LBNP hypovolemic model.<sup>15,16</sup> The prototype University of Massachusetts Medical School (UMMS) system in the reported studies utilized a dual sensor arrangement and mathematical algorithms to eliminate spectral interference from superficial skin and fat regions, and accounts for the variation in light scattering and water when tissue hemoglobin oxygen saturation is calculated. The UMMS system showed superior sensitivity in detecting early changes in central blood volume compared with standard NIR spectroscopy methods.<sup>15,16</sup> On the other hand, broadband DOS simultaneously measures tissue light scattering properties affected by vasoconstriction and changes in intravascular hematocrit, and as a result, absolute concentrations of tissue chromophores ([OHb], [RHb], and [THb]) can be obtained, which is not available with the UMMS system yet. Tissue hemoglobin oxygen saturation ( $S_tO_2$ ) is calculated from [OHb] and [THb] as well. Quantification of tissue chromophore concentrations not only renders the composition of probed tissue volumes (via water and lipid fraction), but also allows insights on tissue perfusion from oxyhemoglobin and deoxyhemoglobin separately, rather than tissue oxygen saturation, which is the function of both oxy- and deoxyhemoglobin. This concept is demonstrated in Figs. 4 and 5(a), where fOHb correlates closely with the decrease in SV, despite a smaller dynamic range of  $S_tO_2$  changes that occur when the oxy- and deoxyhemoglobin concentrations change in the same direction.

There are a number of limitations in this study. The current broadband DOS prototype we used is limited by a single source detector reflectance configuration, and it does not separate

the effects of superficial skin and fat regions in the interrogation field as with the UMMS system, which might behave very differently during hemorrhage compared to the deeper muscle tissue assessed preferentially by the prototype UMMS system.<sup>15,16,55,56</sup> However, broadband DOS systems with multidistance source/detector probes to make analogous tissue layer corrections are under development.<sup>57</sup> While the LBNP model has been shown to provide extensive real-time, continuous data on changes regarding important physiologic variables,<sup>15,16,18,25,34,54</sup> cardiovascular responses to experimentally induced central hypovolemia may be different when compared with physiologic responses to actual severe hemorrhage. As previously discussed, although LBNP causes fluid redistribution from the upper to lower body instead of inducing actual blood loss, previous trials have demonstrated that many of the physiological responses to LBNP are analogous to responses occurring in actual volume loss.<sup>34,58,59</sup> The laboratory induction of controlled central hypovolemia assesses reduced central volume without confounding factors such as tissue injury and painful stimuli that might affect peripheral vascular responses assessed by broadband DOS.

DOS measures tissue-volume-averaged hemoglobin and hemoglobin subfraction concentrations, and thus reflects a combination of tissue vascular volume as well as intravascular hemoglobin concentrations. Thus, in clinical situations that can be frequently encountered in trauma or critical care settings (where changes in vascular volume and intravascular hemoglobin do not always parallel each other), DOS measurements may become difficult to interpret. DOS capabilities would need to be specifically studied in cases where these findings might be expected, such as: 1. when simultaneous vasodilatation from thermal injury or sepsis occurs in the setting of hemorrhage and decreased central volume, or 2. if hypoxemia from lung injury accompanies hemorrhage and resuscitation.

The current system measures only one peripheral site in the current configuration. Regional variability, local traumatic injury, ischemia, or hemorrhage at the site of measurement, or specific organ dysfunction, would not be detected or would otherwise affect measurements with the current design. Future designs of DOS device prototypes with collection in parallel from a number of source/detection channel sites could improve the quality and practicality of multisite data collection.

## 5 Conclusions

While there are a number of limitations in the current study, these promising initial findings suggest that noninvasive DOS measurements may be useful for detection of early changes occurring during hemorrhage and central hypovolemia. If confirmed in clinical settings, such findings could be used to help identify patients requiring more aggressive intervention. Future studies will be needed to compare the sensitivity and specificity of quantitative noninvasive DOS technologies to current clinical technologies, and to recently described UMMS as complementary or competing methods in actual field settings.

## Acknowledgments

The authors thank the subjects for their cheerful cooperation, and Gary Muniz for his engineering and technical assistance during the experiments. This research was supported by funding from the United States Army Medical

Research and Materiel Command Combat Casualty Research Program, AF-9550-04-1-0101, FOS-2004-0011A and 0012A, and LAMMP 445474-30136.

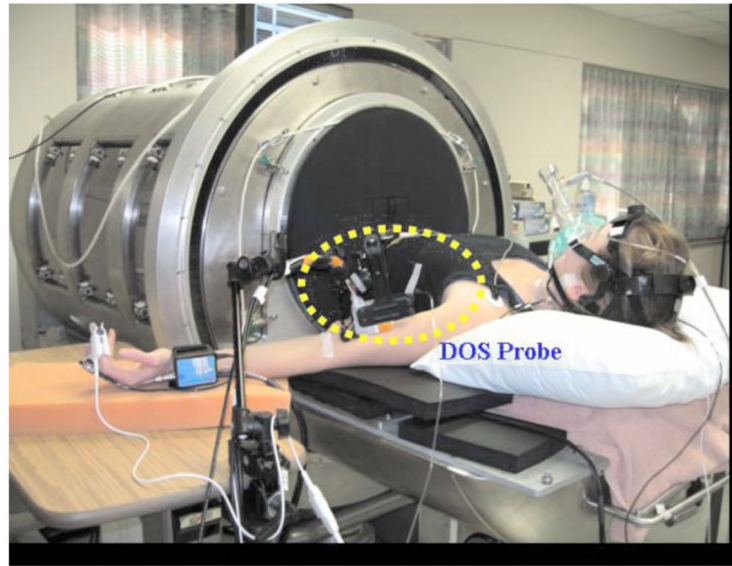
## References

1. Sauaia A, Moore FA, Moore EE, Moser KS, Brennan R, Read RA, Pons PT. Epidemiology of trauma deaths: a reassessment. *J. Trauma*. 1995; 38(2):185–193. [PubMed: 7869433]
2. Bellamy RF. The causes of death in conventional land warfare: implications for combat casualty care research. *Mil. Med*. 1984; 149(2):55–62. [PubMed: 6427656]
3. Champion HR, Sacco WJ, Carnazzo AJ, Copes W, Fouty WJ. Trauma score. *Crit. Care Med*. 1981; 9(9):672–676. [PubMed: 7273818]
4. Champion HR, Sacco WJ, Copes WS, Gann DS, Gennarelli TA, Flanagan ME. A revision of the trauma score. *J. Trauma*. 1989; 29(5):623–629. [PubMed: 2657085]
5. Orlinsky M, Shoemaker W, Reis ED, Kerstein MD. Current controversies in shock and resuscitation. *Surg. Clin. North Am*. 2001; 81(6):1217–1262. xi–xii. [PubMed: 11766174]
6. Mullins RJ, Veum-Stone J, Helfand M, Zimmer-Gembeck M, Hedges JR, Southard PA, Trunkey DD. Outcome of hospitalized injured patients after institution of a trauma system in an urban area. *JAMA, J. Am. Med. Assoc*. 1994; 271(24):1919–1924.
7. Zimmer-Gembeck MJ, Southard PA, Hedges JR, Mullins RJ, Rowland D, Stone JV, Trunkey DD. Triage in an established trauma system. *J. Trauma*. 1995; 39(5):922–928. [PubMed: 7474009]
8. Hedges JR, Feero S, Moore B, Haver DW, Shultz B. Comparison of prehospital trauma triage instruments in a semirural population. *J. Emerg. Med*. 1987; 5(3):197–208. [PubMed: 3429813]
9. Phillips JA, Buchman TG. Optimizing prehospital triage criteria for trauma team alerts. *J. Trauma*. 1993; 34(1):127–132. [PubMed: 8437179]
10. Baxt WG, Berry CC, Epperson MD, Scalzitti V. The failure of prehospital trauma prediction rules to classify trauma patients accurately. *Ann. Emerg. Med*. 1989; 18(1):1–8. [PubMed: 2642672]
11. Baxt WG, Jones G, Fortlage D. The trauma triage rule: a new, resource-based approach to the prehospital identification of major trauma victims. *Ann. Emerg. Med*. 1990; 19(12):1401–1406. [PubMed: 2240753]
12. McManus J, Yershov AL, Ludwig D, Holcomb JB, Salinas J, Dubick MA, Convertino VA, Hinds D, David W, Flanagan T, Duke JH. Radial pulse character relationships to systolic blood pressure and trauma outcomes. *Prehosp Emerg. Care*. 2005; 9(4):423–428. [PubMed: 16263676]
13. Emerman CL, Shade B, Kubincanek J. Comparative performance of the Baxt Trauma Triage Rule. *Ann. Emerg. Med*. 1992; 10(4):294–297.
14. Wo CC, Shoemaker WC, Appel PL, Bishop MH, Kram HB, Hardin E. Unreliability of blood pressure and heart rate to evaluate cardiac output in emergency resuscitation and critical illness. *Crit. Care Med*. 1993; 21(2):218–223. [PubMed: 8428472]
15. Soller BR, Yang Y, Soyemi OO, Ryan KL, Rickards CA, Walz JM, Heard SO, Convertino VA. Noninvasively determined muscle oxygen saturation is an early indicator of central hypovolemia in humans. *J. Appl. Physiol*. 2008; 104(2):475–481. [PubMed: 18006869]
16. Soller BR, Ryan KL, Rickards CA, Cooke WH, Yang Y, Soyemi OO, Crookes BA, Heard SO, Convertino VA. Oxygen saturation determined from deep muscle, not thenar tissue, is an early indicator of central hypovolemia in humans. *Crit. Care Med*. 2008; 36(1):176–182. [PubMed: 18090350]
17. Gosain A, Rabkin J, Reymond JP, Jensen JA, Hunt TK, Upton RA. Tissue oxygen tension and other indicators of blood loss or organ perfusion during graded hemorrhage. *Surgery (St. Louis)*. 1991; 109(4):523–532.
18. Convertino VA, Cooke WH, Holcomb JB. Arterial pulse pressure and its association with reduced stroke volume during progressive central hypovolemia. *J. Trauma*. 2006; 61(3):629–634. [PubMed: 16966999]
19. Batchinsky AI, Cancio LC, Salinas J, Kuusela T, Cooke WH, Wang JJ, Boehme M, Convertino VA, Holcomb JB. Prehospital loss of R-to-R interval complexity is associated with mortality in trauma patients. *J. Trauma*. 2007; 63(3):512–518. [PubMed: 18073594]

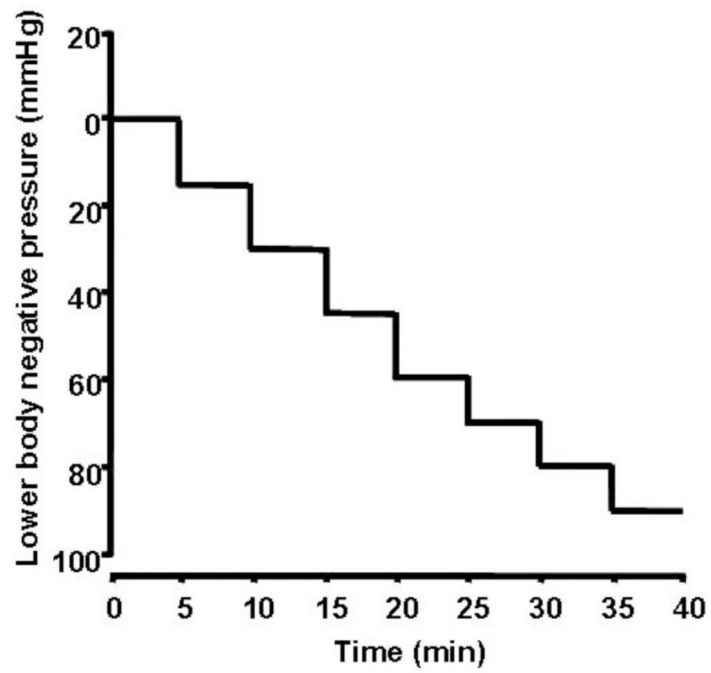
20. Baron BJ, Dutton RP, Zehtabchi S, Spanfelner J, Stavile KL, Khodorkovsky B, Nagdev A, Hahn B, Scalea TM. Sublingual capnometry for rapid determination of the severity of hemorrhagic shock. *J. Trauma*. 2007; 62(1):120–124. [PubMed: 17215742]
21. Donald MJ, Paterson B. End tidal carbon dioxide monitoring in prehospital and retrieval medicine: a review. *Emerg. Med. J.* 2006; 23(9):728–730. [PubMed: 16921096]
22. Dubin A, Murias G, Estenssoro E, Canales H, Sottile P, Badie J, Baran M, Rossi S, Laporte M, Palizas F, Giampieri J, Mediavilla D, Vacca E, Botta D. End-tidal CO<sub>2</sub> pressure determinants during hemorrhagic shock. *Intensive Care Med.* 2000; 26(11):1619–1623. [PubMed: 11193267]
23. Jin X, Weil MH, Tang W, Povoas H, Pernat A, Xie J, Bisera J. End-tidal carbon dioxide as a noninvasive indicator of cardiac index during circulatory shock. *Crit. Care Med.* 2000; 28(7): 2415–2419. [PubMed: 10921572]
24. Cooke WH, Salinas J, Convertino VA, Ludwig DA, Hinds D, Duke JH, Moore FA, Holcomb JB. Heart rate variability and its association with mortality in prehospital trauma patients. *J. Trauma*. 2006; 60(2):363–370. discussion 370. [PubMed: 16508497]
25. Reisner A, Xu D, Ryan K, Convertino V, Mukkamala R. Comparison of cardiac output monitoring methods for detecting central hypovolemia due to lower body negative pressure. *Conf. Proc. IEEE Eng. Med. Biol. Soc.* 2007; 1:955–958. [PubMed: 18002116]
26. Tromberg, BJ.; Coquoz, O.; Fishkin, JB.; Anderson, ER.; Pham, D.; Brenner, M.; Svaasand, LO. Frequency-Domain Photon Migration (FDPM) Measurements of Normal and Malignant Cell and Tissue Optical Properties. Sevick-Muraca, E.; Benaron, D., editors. 1996. p. 111-116.
27. Pham TH, Coquoz O, Fishkin JB, Anderson E, Tromberg BJ. Broad bandwidth frequency domain instrument for quantitative tissue optical spectroscopy. *Rev. Sci. Instrum.* 2000; 71(6):2500–2513.
28. Albert C, Richard Van W, Feizal W, Bruce T. Noninvasive monitoring of red blood cell transfusion in very low birthweight infants using diffuse optical spectroscopy. *J. Biomed. Opt.* 2005; 10(5):051401. [PubMed: 16292938]
29. Lee J, El-Abaddi N, Duke A, Cerussi AE, Brenner M, Tromberg BJ. Noninvasive in vivo monitoring of methemoglobin formation and reduction with broadband diffuse optical spectroscopy. *J. Appl. Physiol.* 2006; 100(2):615–622. [PubMed: 16223982]
30. Lee J, Saltzman DJ, Cerussi AE, Gelfand DV, Milliken J, Waddington T, Tromberg BJ, Brenner M. Broadband diffuse optical spectroscopy measurement of hemoglobin concentration during hypovolemia in rabbits. *Physiol. Meas.* 2006; 27(8):757–767. [PubMed: 16772673]
31. Lee J, Cerussi AE, Saltzman D, Waddington T, Tromberg BJ, Brenner M. Hemoglobin measurement patterns during noninvasive diffuse optical spectroscopy monitoring of hypovolemic shock and fluid replacement. *J. Biomed. Opt.* 2007; 12(2):024001. [PubMed: 17477716]
32. Pham T, Coquoz O, Fishkin J, Anderson EA, Tromberg BJ. A broad bandwidth frequency domain instrument for quantitative tissue optical spectroscopy. *Rev. Sci. Instrum.* 2000; 71(6):1–14.
33. Pham TH, Hornung R, Ha HP, Burney T, Serna D, Powell L, Brenner M, Tromberg BJ. Noninvasive monitoring of hemodynamic stress using quantitative near-infrared frequency-domain photon migration spectroscopy. *J. Biomed. Opt.* 2002; 7(1):34–44. [PubMed: 11818010]
34. Cooke WH, Ryan KL, Convertino VA. Lower body negative pressure as a model to study progression to acute hemorrhagic shock in humans. *J. Appl. Physiol.* 2004; 96(4):1249–1261. [PubMed: 15016789]
35. McManus JG, Convertino VA, Cooke WH, Ludwig DA, Holcomb JB. R-wave amplitude in lead II of an electrocardiograph correlates with central hypovolemia in human beings. *Acad. Emerg. Med.* 2006; 13(10):1003–1010. [PubMed: 16973639]
36. Convertino VA, Ryan KL, Rickards CA, Cooke WH, Idris AH, Metzger A, Holcomb JB, Adams BD, Lurie KG. Inspiratory resistance maintains arterial pressure during central hypovolemia: implications for treatment of patients with severe hemorrhage. *Crit. Care Med.* 2007; 35(4):1145–1152. [PubMed: 17334239]
37. Rickards CA, Ryan KL, Cooke WH, Lurie KG, Convertino VA. Inspiratory resistance delays the reporting of symptoms with central hypovolemia: association with cerebral blood flow. *Am. J. Physiol. Regulatory Integrative Comp. Physiol.* 2007; 293(1):R243–R250.

38. Imholz BP, van Montfrans GA, Settels JJ, van der Hoeven GM, Karemaker JM, Wieling W. Continuous non-invasive blood pressure monitoring: reliability of Finapres device during the Valsalva manoeuvre. *Cardiovasc. Res.* 1988; 22(6):390–397. [PubMed: 3224351]
39. Parati G, Casadei R, Groppelli A, Di Rienzo M, Mancia G. Comparison of finger and intra-arterial blood pressure monitoring at rest and during laboratory testing. *Hypertension.* 1989; 13(6 pt 1): 647–655. [PubMed: 2500393]
40. Dorlas JC, Nijboer JA, Butijn WT, van der Hoeven GM, Settels JJ, Wesseling KH. Effects of peripheral vasoconstriction on the blood pressure in the finger, measured continuously by a new noninvasive method (the Finapres). *Anesthesiology.* 1985; 62(3):342–345. [PubMed: 3977117]
41. Newman DG, Callister R. The non-invasive assessment of stroke volume and cardiac output by impedance cardiography: a review. *Aviat., Space Environ. Med.* 1999; 70(8):780–789. [PubMed: 10447052]
42. Kubicek WG, Karnegis JN, Patterson RP, Witsoe DA, Mattson RH. Development and evaluation of an impedance cardiac output system. *Aerosp. Med.* 1966; 37(12):1208–1212. [PubMed: 5339656]
43. Cerussi A, Hsiang D, Shah N, Mehta R, Durkin A, Butler J, Tromberg BJ. Predicting response to breast cancer neoadjuvant chemotherapy using diffuse optical spectroscopy. *Proc. Natl. Acad. Sci. U.S.A.* 2007; 104(10):4014–4019. [PubMed: 17360469]
44. Bevilacqua F, Berger AJ, Cerussi AE, Jakubowski D, Tromberg BJ. Broadband absorption spectroscopy in turbid media by combined frequency-domain and steady-state methods. *Appl. Opt.* 2000; 39(34):6498–6507. [PubMed: 18354663]
45. Tromberg BJ, Cerussi A, Shah N, Compton M, Durkin A, Hsiang D, Butler J, Mehta R. Imaging in breast cancer: diffuse optics in breast cancer: detecting tumors in pre-menopausal women and monitoring neoadjuvant chemotherapy. *Breast Cancer Res. Treat.* 2005; 7(6):279–285.
46. Bevilacqua F, Berger AJ, Cerussi AE, Jakubowski D, Tromberg BJ. Broadband absorption spectroscopy in turbid media by combined frequency-domain and steady-state methods. *Appl. Opt.* 2000; 39(34):6498–6507. [PubMed: 18354663]
47. Tromberg BJ, Shah N, Lanning R, Cerussi A, Espinoza J, Pham T, Svaasand L, Butler J. Non-invasive in vivo characterization of breast tumors using photon migration spectroscopy. *Neoplasia.* 2000; 2(1–2):26–40. [PubMed: 10933066]
48. Pham TH, Coquoz O, Fishikina JB, Anderson E, Tromberg BJ. Broad bandwidth frequency domain instrument for quantitative tissue optical spectroscopy. *Rev. Sci. Instrum.* 2000; 71:2500–2513.
49. Graaff R, Aarnoose JG, Zijp JR, Sloot PMA, de Mul FFM, Greve J, Koelink MH. Reduced light-scattering properties for mixtures of spherical particles: a simple approximation derived from Mie calculation. *Appl. Opt.* 1992; 31:1370–1376. [PubMed: 20720767]
50. Mourant JR, Fuselier T, Boyer J, Johnson T, Bigio IJ. Predictions and measurements of scattering and absorption over broad wavelength ranges in tissue phantoms. *Appl. Opt.* 1997; 36:949–957. [PubMed: 18250760]
51. Schmitt JM, Kumar G. Optical scattering properties of soft tissue: a discrete particle model. *Appl. Opt.* 1998; 37:2788–2797. [PubMed: 18273225]
52. Zijlstra, WG.; Buursma, A.; Assendelft, OW. *Visible and Near-Infrared Absorption Spectra of Human and Animal Hemoglobin.* Netherlands: VSP BV, AH Zeist; 2000.
53. Sather TM, Goldwater DJ, Montgomery LD, Convertino VA. Cardiovascular dynamics associated with tolerance to lower body negative pressure. *Aviat., Space Environ. Med.* 1986; 57(5):413–419. [PubMed: 3707470]
54. Convertino VA. Gender differences in autonomic functions associated with blood pressure regulation. *Am. J. Physiol.* 1998; 275(6 pt 2):R1909–R1920. [PubMed: 9843880]
55. Gutierrez G, Reines HD, Wulf-Gutierrez ME. Clinical review: hemorrhagic shock. *Crit. Care.* 2004; 8(5):373–381. [PubMed: 15469601]
56. Yang Y, Soyemi O, Scott P, Landry M, Lee S, Stroud L, Soller B. Quantitative measurement of muscle oxygen saturation without influence from skin and fat using continuous-wave near infrared spectroscopy. *Opt. Express.* 2007; 15(21):13715–13720. [PubMed: 19550643]

57. Li A, Kwong R, Cerussi A, Merritt S, Hayakawa C, Tromberg BJ. Method for recovering quantitative broadband diffuse optical spectra from layered media. *Appl. Opt.* 2007; 46(21):4828–4833. [PubMed: 17609733]
58. Geeraerts T, Albaladejo P, Declere AD, Duranteau J, Sales JP, Benhamou D. Decrease in left ventricular ejection time on digital arterial waveform during simulated hypovolemia in normal humans. *J. Trauma.* 2004; 56(4):845–849. [PubMed: 15187752]
59. Taneja I, Moran C, Medow MS, Glover JL, Montgomery LD, Stewart JM. Differential effects of lower body negative pressure and upright tilt on splanchnic blood volume. *Am. J. Physiol. Heart Circ. Physiol.* 2007; 292(3):H1420–H1426. [PubMed: 17085534]



(a)



(b)

**Fig. 1.** (a) Subject in the lower body negative pressure (LBNP) and (b) the standard LBNP protocol.

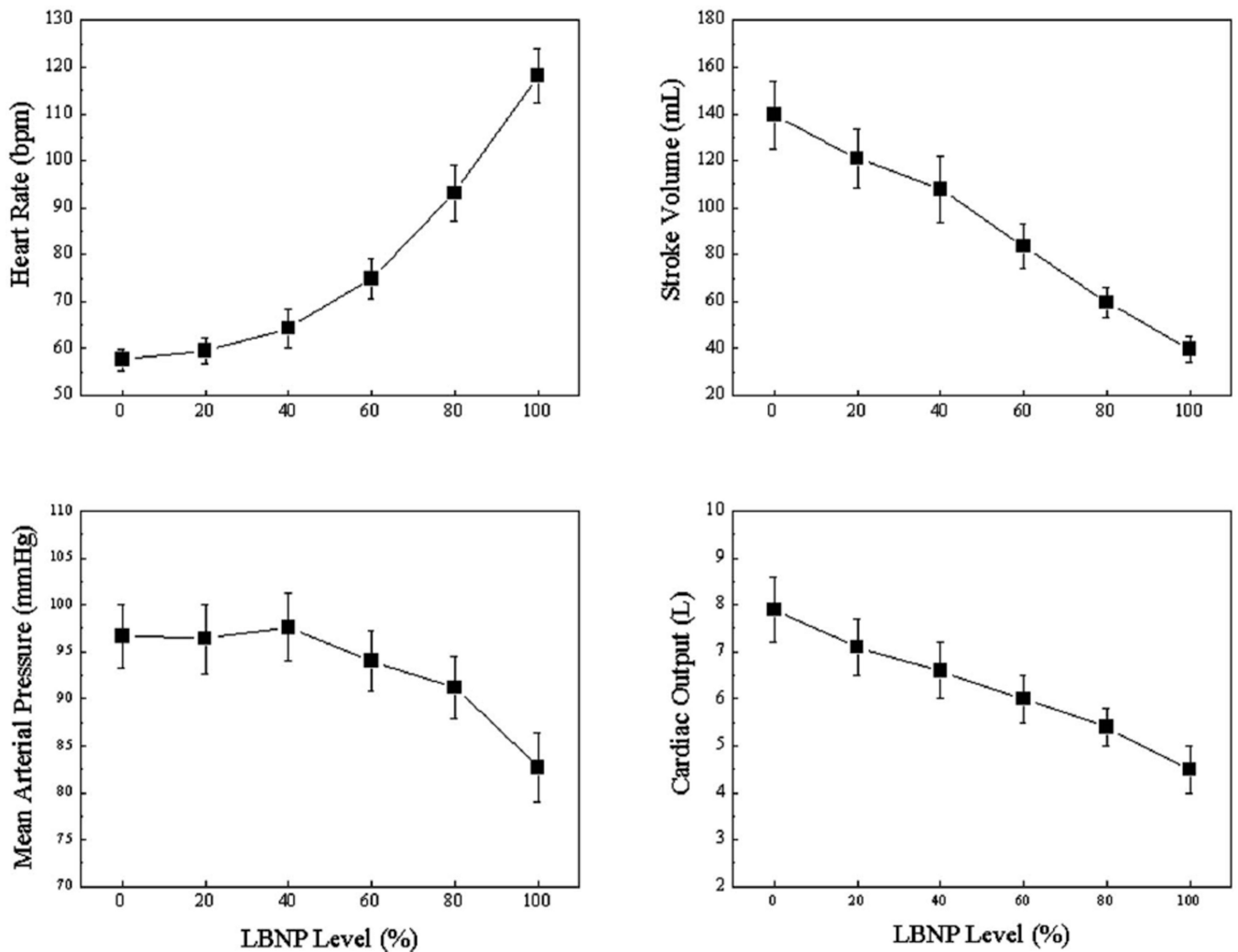


**Fig. 2.** Heart rate, mean arterial pressure, stroke volume, and cardiac output throughout the lower body negative pressure (LBNP) protocol. Due to intersubject variation in LBNP time to hemodynamic decompensation, responses to LBNP were reapportioned to equal fractions between 0% LBNP tolerance (baseline) and 100% LBNP tolerance, the level where hemodynamic decompensation occurred and the LBNP terminated. Data are from all ten subjects and are presented as mean  $\pm$  standard error (SE).



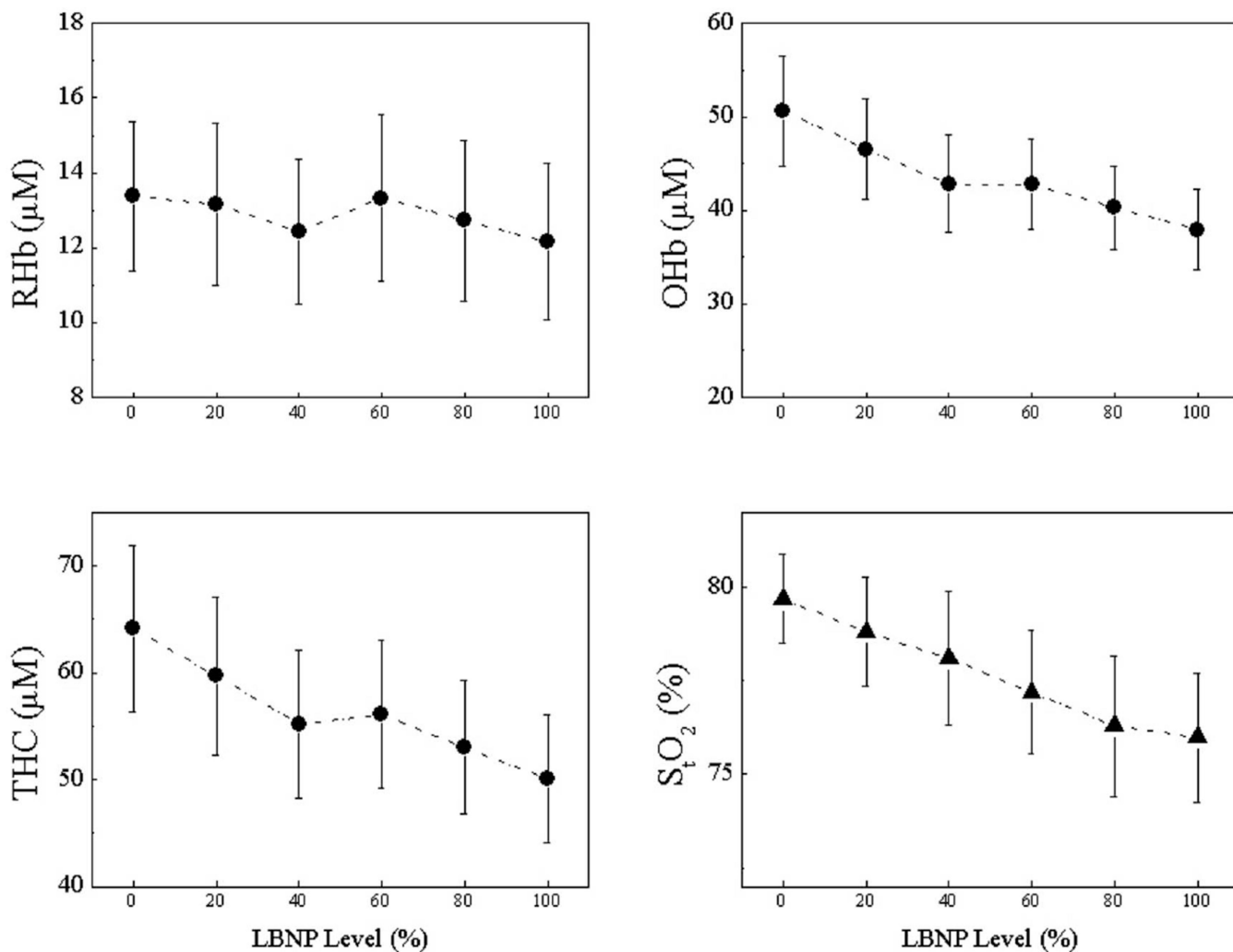


**Fig. 3.** Absolute concentrations of deoxyhemoglobin (RHb), oxyhemoglobin (OHb), and total hemoglobin (THb) and tissue hemoglobin O<sub>2</sub> saturation (StO<sub>2</sub>) throughout the lower body negative pressure (LBNP) protocol. Data are from all ten subjects and are presented as mean  $\pm$  standard error (SE).

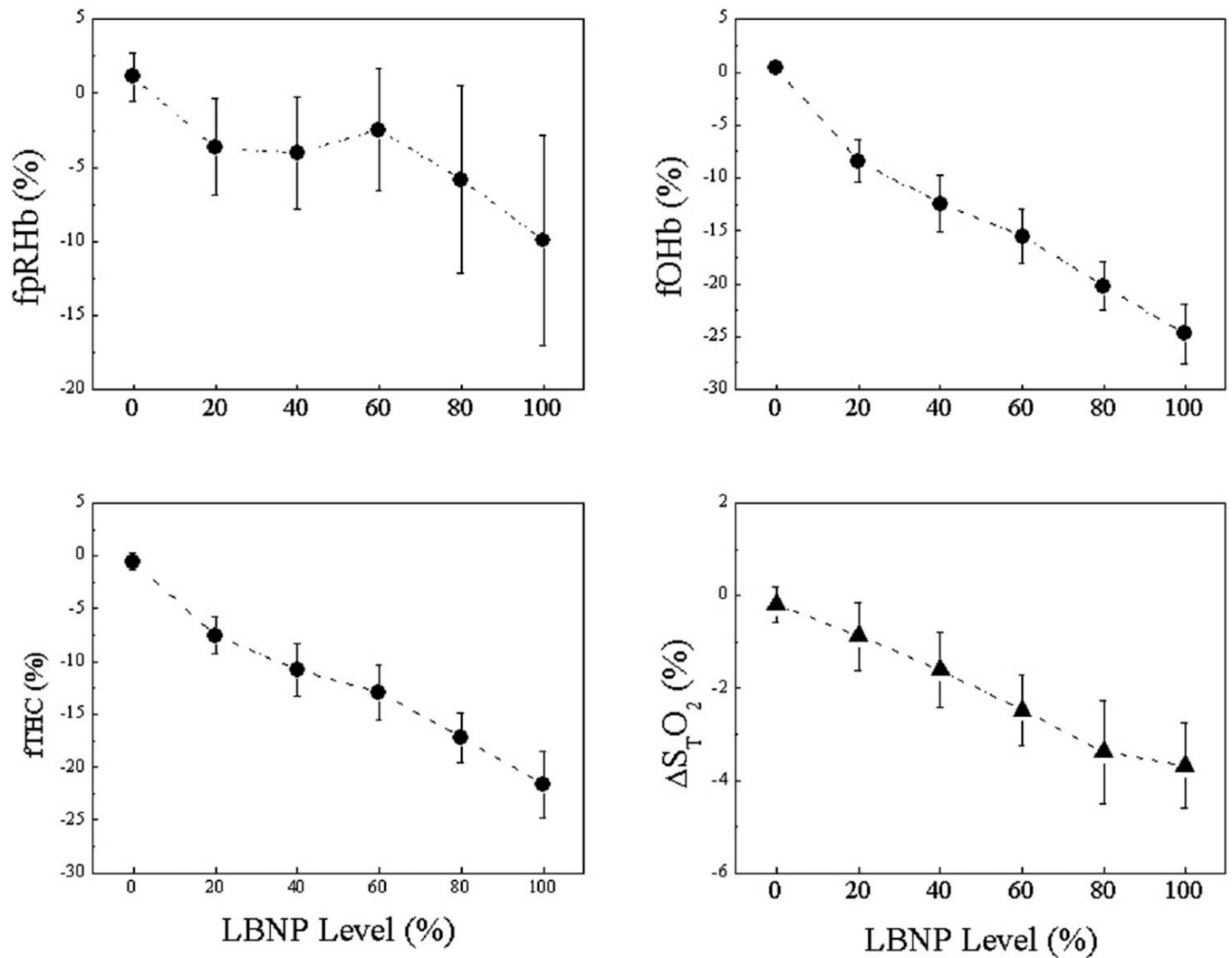
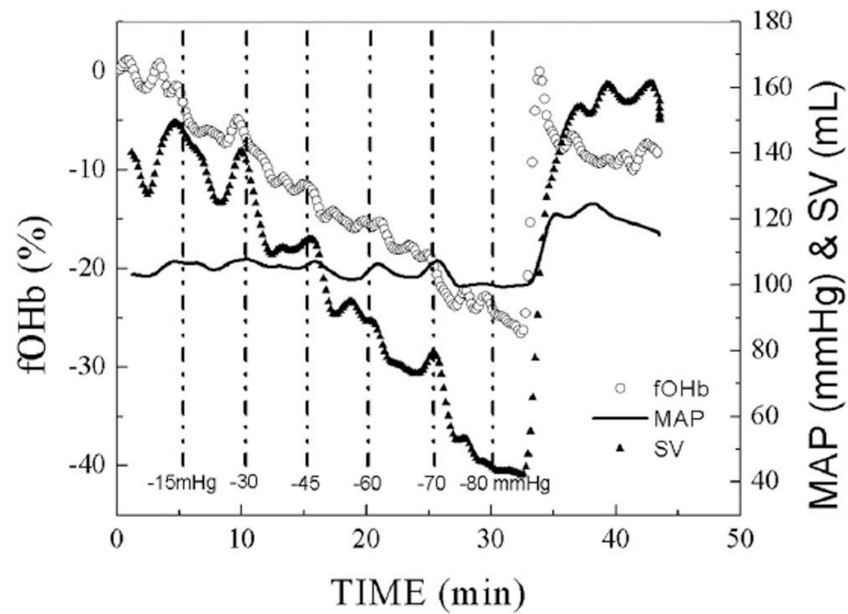
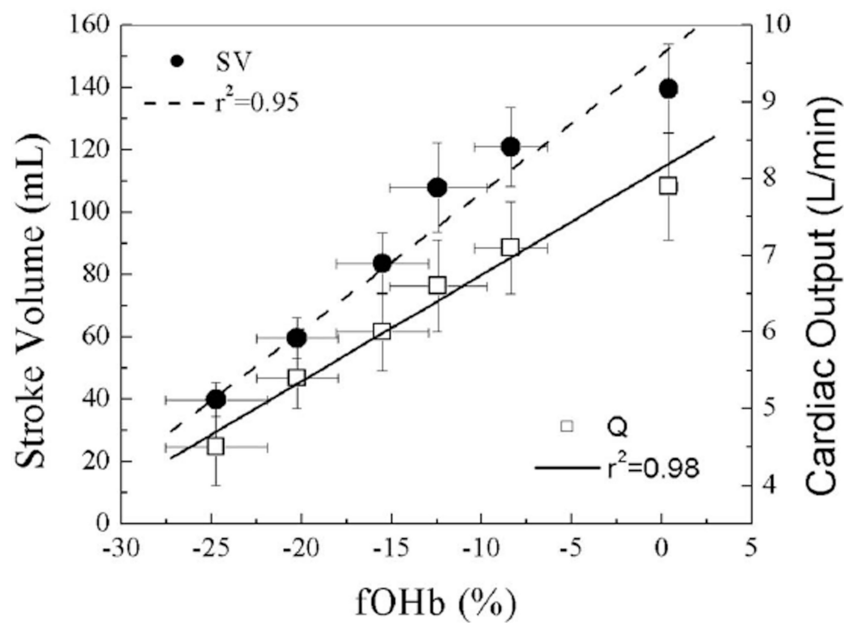


**Fig. 4.** Fractional changes in concentrations of deoxyhemoglobin, oxyhemoglobin, and total hemoglobin and changes in tissue hemoglobin  $O_2$  saturation throughout the lower body negative pressure (LBNP) protocol. Data are from all ten subjects and are presented as mean  $\pm$  standard error (SE).



(a)



(b)

**Fig. 5.**

(a) Time course plots of DOS fOHb, mean arterial pressure, and stroke volume from a single subject (male, 24 yr, 191 cm, 73 kg). The subject experienced presyncope during a  $-80$ -mmHg LBNP. Dash-dot lines represent the time points where new LBNP levels were applied. Mean arterial pressure and stroke volume data points were extracted from a continual Finometer measurement, and synchronized with DOS fOHb data points for the illustrative comparison only. (b) Changes in stroke volume (left y axis) and cardiac output (right y axis) plotted against changes in fOHb during LBNP. Data represent the average

values at specific LBNP levels and error bars represent standard errors. Data are from all ten subjects and are presented as mean $\pm$ standard error (SE).

**Table 1**

Absolute values of heart rate (HR), mean arterial pressure (MAP), stroke volume (SV), cardiac output (Q), oxyhemoglobin (OHb), deoxyhemoglobin (RHb), total hemoglobin (THb), and tissue O<sub>2</sub> saturation (StO<sub>2</sub>) at baseline and at 100% LBNP tolerance. indicates the absolute changes from the baseline values, while f\_ indicates the percentage changes relative to the baseline values.

	Baseline	100% LBNP Tolerance	p value
Heart rate (beats/min)	57.6±2.3	104±3	<0.001
Mean arterial pressure (mmHg)	96.7±3.4	73±1	0.012
Stroke volume (ml)	139.5±14.3	84±2	<0.001
Cardiac output (l/min)	7.9±0.7	4.5±0.5	<0.001*
Lipid fraction (%)	46.3±5.5	48.2±5.3	0.464
Water fraction (%)	49.2±5.9	48.3±5.1	0.684
Oxyhemoglobin (µM)	50.6±5.9	37.9±4.3	0.098
Deoxyhemoglobin (µM)	13.4±2.0	12.2±2.1	0.678
Total hemoglobin (µM)	64.1±7.8	50.1±6.0	0.171*
Tissue O <sub>2</sub> saturation (%)	79.7±1.2	76.0±1.7	0.095*
Tissue O <sub>2</sub> saturation (%)	-0.1±0.2	-3.9±0.9	<0.001*
f <sub>oxy</sub> hemoglobin (%)	0.5±0.3	-24.7±2.8	<0.001
f <sub>deoxy</sub> hemoglobin (%)	0.8±0.9	-9.9±7.1	0.150
f <sub>total</sub> hemoglobin (%)	-0.3±0.4	-21.6±3.2	<0.001*

\* Q, THb, and StO<sub>2</sub> are derived variables.

**Table 2**

Simple Pearson correlation coefficients ( $r^2$ ) between LBNP and DOS parameters. Stroke volume (SV) and cardiac output (Q) are from electric impedance measurements.

	<b>RHb</b>	<b>OHb</b>	<b>S<sub>t</sub>O<sub>2</sub></b>	<b>THb</b>	<b>S<sub>t</sub>O<sub>2</sub></b>	<b>fRHb</b>	<b>fOHb</b>	<b>fTHb</b>
HR	0.50	0.74	0.82	0.74	0.84	0.77	0.80	0.83
MAP	0.40	0.57	0.65	0.57	0.67	0.70	0.64	0.68
SV	0.45	0.90	0.98	0.88	0.98	0.77	0.95	0.96
Q	0.51	0.94	0.97	0.93	0.97	0.83	0.98	0.98